

Entanglement as a topological marker in harmonically confined attractive Fermi-Hubbard chains

M. Sanino, I. M. Carvalho, and V. V. França

São Paulo State University (UNESP), Institute of Chemistry, 14800-090, Araraquara, São Paulo, Brazil

We investigate the single-site von Neumann entropy along a harmonically confined superfluid chain, as described by the one-dimensional fermionic Hubbard model with strongly attractive interactions. We find that by increasing the confinement (or equivalently the particle filling) the system undergoes a quantum phase transition from a superfluid (SF) to a non-trivial topological insulator (TI) phase, which is characterized by an insulating bulk surrounded by highly entangled superfluid edges. These highly entangled states are found to be robust against perturbations and topologically protected by the particle-hole symmetry, which is locally preserved. We also find a semi-quantitative agreement between entanglement and superconducting order parameter profiles, confirming then that entanglement can be used as a topological marker and an order parameter in these systems. The charge gap not only confirms the SF-TI transition, but also shows that this transition is mediated by a metallic intermediate regime within the bulk. Using the gap we could depict a phase diagram for which the non-trivial topological insulator can be found in such harmonically confined attractive systems.

I. INTRODUCTION

Topological states have received interest across various physical systems due to their unique properties, such as robustness against local perturbations and disorder^{1–7}. These properties not only deepen our understanding of quantum materials, but can also be used in practical applications, including fault-tolerant quantum computing and novel electronic or photonic devices^{8–10}.

While noninteracting topological states are in many cases well described using topological band theory¹¹, based on the assumption of perfect translational symmetry^{12,13}, obtaining topological invariants for interacting systems without translational symmetry – as harmonically confined cold-atom systems – becomes challenging^{14–17}. In two-dimensional systems a local Chern number has been proposed as a topological marker in coordinate space¹⁵, while a similar approach has been proposed to the Boltzmann entropy for the three-dimensional optical lattices¹⁸.

State-of-the-art experiments with ultracold atoms in optical lattices^{19,20} represent a strategic resource for simulating quantum many-body phenomena, as they allow the replication of complex quantum models in a highly tunable environment. For example, one-dimensional (1D) optical lattices can be engineered to precisely realize the fermionic 1D Hubbard model²¹, where two hyperfine states interact via an onsite potential and are subject to harmonic confinement.

In the context of quantum phase transitions, entanglement has been demonstrated to be a powerful tool^{22–29} since it captures fundamental nonlocal correlations in quantum many-body systems. At a quantum phase transition, the ground state of a system changes qualitatively due to quantum fluctuations, and these changes are often reflected in the structure of entanglement. Therefore, it is natural to have interest in using entanglement as a probe to detect the topological properties of many-body quantum states^{30–32}. For example, the entanglement spectrum has been used to fingerprint topological order^{33–35}. In Kitaev materials spin-orbit entanglement actually leads to topological phases³⁶. Entanglement entropy has

also been used to determine topological order in spin-liquid phase in a Bose–Hubbard model on the Kagome lattice³⁷.

Here we explore the single-site von Neumann entropy along a harmonically confined chain described by the 1D Hubbard model in the strongly attractive regime. This *entanglement profile* – which to our knowledge has never been used to characterize quantum phase transitions – has the potential to directly probe the non-trivial topological structure within the system. We find that by increasing the harmonic strength (or equivalently by increasing the particle filling), the system undergoes a transition from a superfluid to a non-trivial topological insulator, characterized by an insulating bulk surrounded by highly entangled superfluid edges. We show that these highly entangled superfluid edges are robust against perturbations and are topologically protected by the particle-hole symmetry, which is locally preserved. The charge gap not only confirms our interpretation but also reveal an intermediate metallic phase, allowing us to depict a phase diagram for superfluid, metal and non-trivial topological insulator phases as a function of density and confinement. The entanglement profile is also found to be semi-quantitatively equivalent to the superconducting order parameter profile, confirming then that entanglement can be used as a topological marker and an order parameter in these systems.

II. MODEL AND METHODS

We consider 1D fermionic Hubbard³⁸ chains under harmonic confinement, described by the Hamiltonian

$$\hat{H} = -t \sum_{i=1,\sigma}^{L-1} (\hat{c}_{i,\sigma}^\dagger \hat{c}_{i+1,\sigma} + \text{H.c.}) + U \sum_{i=1}^L \hat{n}_{i,\uparrow} \hat{n}_{i,\downarrow} + k \sum_{i=1,\sigma}^L (i - ((L+1)/2))^2 \hat{n}_{i,\sigma}, \quad (1)$$

where t is the nearest-neighbor hopping term, $U < 0$ is the attractive onsite interaction and k is the curvature of the parabolic potential. Here $\hat{c}_{i,\sigma}^{(\dagger)}$ annihilates (creates) an electron

with spin $\sigma = \uparrow, \downarrow$ at site i , $\hat{n}_{i,\sigma} = \hat{c}_{i,\sigma}^\dagger \hat{c}_{i,\sigma}$ is the number operator and L is the chain size with open boundary conditions. Throughout this work, we set $t = 1$ as the unit of energy. We here focus on strongly attractive interactions, $U = -10$, while the weakly attractive regime, including the BCS limit^{39,40}, will be explored elsewhere.

The ground-state properties are obtained via Density Matrix Renormalization Group (DMRG) methods^{41,42} at a fixed filling $n = N/L$ and balanced spin populations $N_\uparrow = N_\downarrow = N/2$, where $N = \sum_i (\langle \hat{n}_{i,\uparrow} \rangle + \langle \hat{n}_{i,\downarrow} \rangle) = N_\uparrow + N_\downarrow$ is the total number of particles. The DMRG algorithm was implemented using the ITensor Library⁴³, based on the matrix product states (MPS) ansatz⁴¹. The accuracy of the MPS representation is controlled by the bond dimension, which was set to a maximum value of 2048. We initialize the DMRG calculations by configuring an initial state with doubly occupied sites, extending from the middle of the chain towards the boundaries. This approach allows faster convergence, as the target ground state exhibits a similar fermion distribution within the attractive regime. Our calculations were performed until the ground-state energy has converged to at least 10^{-7} .

The density profile $\{\langle \hat{n}_i \rangle\}$ and the occupation probabilities' profiles $\{w_{i2}, w_{i\uparrow}, w_{i\downarrow}, w_{i0}\}$ are directly obtained from the DMRG calculations. Here w_{i2} is the double occupation at site i , $w_{i\sigma}$ the probability of single occupation with σ -spin (for zero magnetization $w_{i\uparrow} = w_{i\downarrow}$), while $w_{i0} = 1 - w_{i\uparrow} - w_{i\downarrow} - w_{i2}$ is the probability of zero occupation.

The single-site entanglement S_i , i.e. the entanglement between site i and the remaining sites in the ground state, is calculated via the von Neumann entropy,

$$\begin{aligned} S_i &= \frac{-1}{\log_2 d} \text{Tr}[\rho_i \log_2 \rho_i] \\ &= \frac{-1}{\log_2 d} [2w_{i\sigma} \log_2 w_{i\sigma} + w_{i2} \log_2 w_{i2} + w_{i0} \log_2 w_{i0}] \end{aligned} \quad (2)$$

where $d = 4$ represents the single-site Hilbert space dimension and $\rho_i = \text{Tr}_{L-i}[\rho]$ is the reduced density matrix of i th site, obtained by tracing out the degrees of freedom of the remaining $L - i$ sites from the total density matrix ρ . In general one has considered the average single-site entanglement, $\bar{S} = 1/L \sum_i S_i$, for detecting quantum phase transitions^{22,44-49}. We here explore instead the entanglement profile $\{S_i\}$, which to our knowledge has never been used to characterize quantum phase transitions, although a similar approach has been proposed to the Boltzmann entropy¹⁸.

We also analyse the superconducting order parameter⁵⁰⁻⁵², defined as

$$\Delta_{pair} = \langle \hat{c}_{i,\downarrow} \hat{c}_{i,\uparrow} \hat{c}_{i+1,\downarrow}^\dagger \hat{c}_{i+1,\uparrow}^\dagger + \text{H.c.} \rangle, \quad (3)$$

which accounts for the pair-pair correlations, and the charge gap,

$$\Delta_c = E_{GS}(N-2) + E_{GS}(N+2) - 2E_{GS}(N), \quad (4)$$

where $E_{GS}(N)$ is the ground-state energy of a system with N fermions with null magnetization.

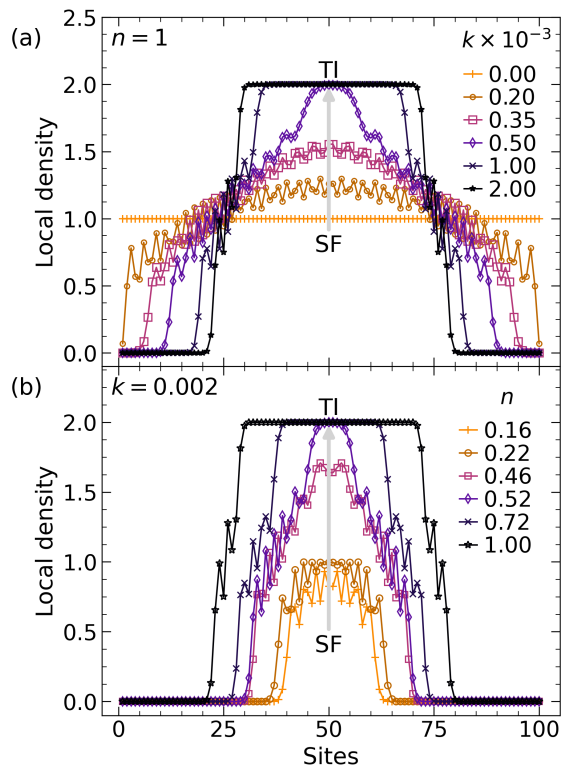


FIG. 1. (a) Effect of the harmonic curvature k on the density profile at fixed $n = 1$. As k increases the effective chain at the core reduces, leading the superfluid (SF) bulk to an insulator phase (topological insulator, TI). As increasing k is equivalent to increase the effective density, this superfluid-insulator transition at the bulk can also be driven by the average density n at a fixed k , as shown in (b) for $k = 0.002$. Here Δ_{pair} was normalized by a factor 0.73, such that it resides between $0 \leq \Delta_{pair} \leq 1$. In all cases $L = 100$ and $U = -10$.

III. RESULTS AND DISCUSSION

We start by considering the effects of the confinement potential on the onsite measurements within a superfluid (SF) sample. Figure 1(a) presents the density profile $\{n_i\}$ for several potential curvatures k at a fixed average density $n = 1$. We find that the flat charge distribution over the entire chain, observed at the superfluid regime ($k = 0$), quickly evolves to a higher concentration of particles at the trap center as the confinement increases. This then defines at the potential core an effective chain^{53,54} (whose size is dependent on k) with an effective higher density, $n_{eff} > n$, while the ends of the chain are kept empty. We also see that for $k \gtrsim 0.0005$ there appears a flat plateau with $n_i = 2$ (fully occupied sites) at the potential center, which becomes broader as k increases further. This fully occupied bulk characterizes a band-like insulator – composed of hardcore bosons such as pure Fock states^{53,55,56} – since within the bulk the charge itinerancy is now totally suppressed. Thus the confinement induces a transition at the bulk from a superfluid to an insulator. Notice that the same superfluid-insulator transition can alternatively be induced by the increase of the average density at a fixed k , Fig. 1(b), as

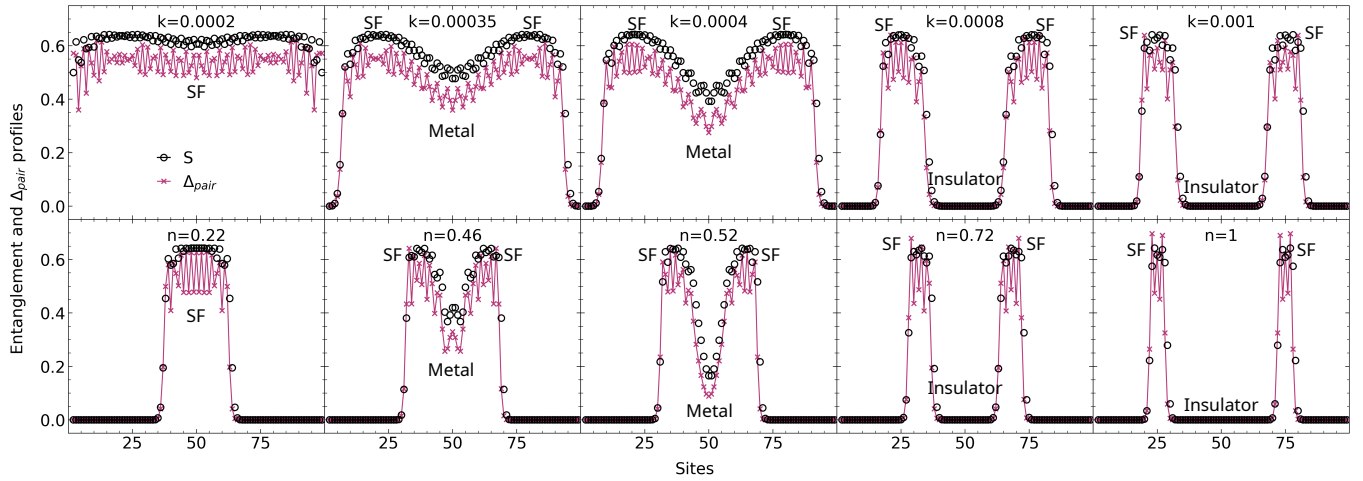


FIG. 2. Entanglement $\{S_i\}$ and superconducting order parameter $\{\Delta_{pair}\}$ profiles for several confinement strengths k at fixed $n = 1$ (upper panels) and for several average densities n at fixed $k = 0.002$ (bottom panels). The initial superfluid (SF), with high entanglement $S_i \sim 0.62$ and $\Delta_{pair} \sim 0.55$ (small k or n), evolves to a metallic phase at the bulk (for increasing k or n), with finite but reduced S_i and Δ_{pair} , keeping superfluid edges; finally reaching (by increasing further k or n) a non-trivial topological insulator (TI), characterized by an insulator bulk surrounded by highly entangled superfluid edges. Notice that both quantities have a semi-quantitative agreement, confirming that entanglement can be used as a topological marker and an order parameter. In all cases $L = 100$ and $U = -10$.

also seen in spin-imbalanced chains⁵³, since it leads equivalently to a higher effective density at the bulk.

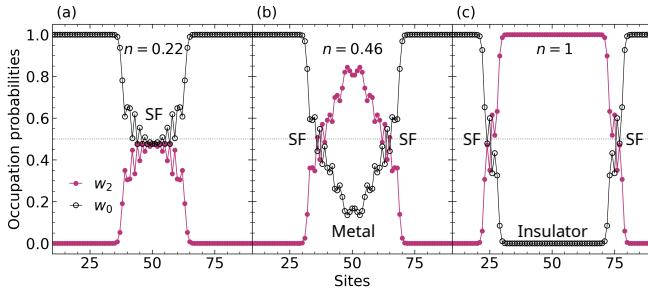


FIG. 3. Double occupancy $\{w_{i2}\}$ and empty-occupation probability $\{w_{i0}\}$ profiles for three distinct average densities within the superfluid (SF), the metallic and the non-trivial topological insulator (TI) regimes. The entanglement at the SF edges is protected by the local particle-hole symmetry ($w_{i2} = w_{i0}$). In all cases $L = 100$, $k = 0.002$ and $U = -10$.

We then analyze this superfluid-insulator transition through both the single-site entanglement and the superconducting order parameter, as shown in Figure 2. For small k (or n) the bulk is a superfluid, characterized by a high superconducting order parameter ($\Delta_{pair} \approx 0.55$) and high entanglement ($S_i \approx 0.62$). As k (or n) increases, the superconducting phase at the bulk is (i) projected towards the edges and (ii) replaced by a metallic phase, marked by a smaller but finite entanglement and a corresponding decrease of the Δ_{pair} . By increasing k (or n) further, the bulk is transformed into an insulator, vanishing both entanglement and Δ_{pair} . Notice that this intermediate metallic regime could not be distinguished from the density profiles presented in Fig. 1. It is also interesting that for all cases both quantities, S_i and Δ_{pair} , are

semi-quantitatively equivalent, thus the single-site entanglement can be considered a semi-quantitative order parameter for the insulator, metallic and superfluid phases within these systems.

The most remarkable feature in Fig. 2 is however the fact that the entanglement is conserved in its high value $S_i \approx 0.62$ for any k (or n): the highly entangled edge states are then robust against perturbations. This robustness of the edge states is a clear signature of symmetry-protected topological phases^{57–59}. The analysis of the double and empty occupation probabilities, in Figure 3, reveal that the symmetry protecting the entanglement at the edges in this system is the particle-hole symmetry, since locally we have $w_2 \sim w_0$. Our findings then show that the superfluid edges are topologically protected by the particle-hole symmetry at the boundaries of the harmonic potential, thus for sufficiently strong confinement the system becomes a *non-trivial topological insulator* (TI), characterized by an insulating bulk – with null S and Δ_{pair} – surrounded by highly entangled superfluid edges. The entanglement profile can be used then as a topological marker in these systems.

The charge gap Δ_c in Figure 4 corroborates our interpretation: for a fixed confinement, there exists a critical n_c for which $\Delta_c \rightarrow 0$, corresponding to the metallic bulk regime. For $n < n_c$ the system is a superfluid, with finite but small gap, resembling the pairing gap⁶⁰, and almost constant with n . While for $n > n_c$ the gap increases almost linearly with n , confirming that the system has reached the non-trivial topological insulator (TI) regime. The phase diagram for the SF, metallic and TI phases can be then depicted via the charge gap, as shows Figure 5. Finally, the analysis of the gap for several chain sizes, Fig. 4, shows that Δ_c reaches small but finite values at the metallic state at n_c in the thermodynamic limit. This fact is crucial for the protection of the non-trivial topological prop-

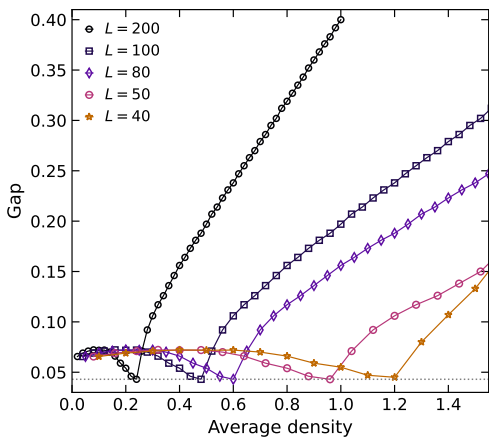


FIG. 4. Charge gap Δ_c as a function of the average density n characterizing: *i*) the superfluid (SF) phase for $n < n_c$, with a small gap independent on n ; *ii*) the metallic intermediate regime, at $n = n_c$, with $\Delta_c \rightarrow 0$; and *iii*) the non-trivial topological insulator (TI) for $n > n_c$, with a larger and increasing with n gap. Notice that increasing L changes n_c and the TI gap, but the SF and the metallic phase gaps are constant and finite in the thermodynamic limit. In all cases $k = 0.002$ and $U = -10$.

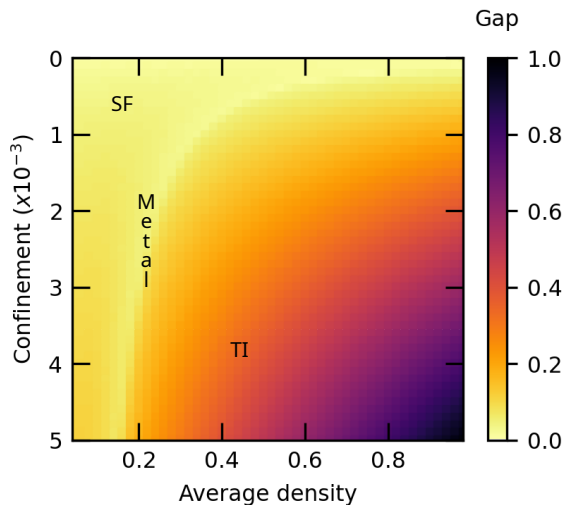


FIG. 5. Phase diagram (depicted via the charge gap for $L = 200$ and $U = -10$) as a function of the confinement strength and average density, demarking the superfluid (SF) phase with finite but small gap, the metallic intermediate regime with $\Delta_c \rightarrow 0$, and the non-trivial topological insulator (TI) phase, with larger gap.

erties, and has also been observed in previous investigations of topological Mott insulator in superlattices⁶¹.

IV. CONCLUSIONS

In summary we have investigated the impact of harmonic confinement on the onsite measurements of strongly attractive superfluids. The density profile signs the superfluid to

insulator transition at the bulk driven by either the confinement strength (at a fixed average density) or the average density (at a fixed confinement). The profiles of single-site entanglement and superconducting order parameter reveal that the superfluid is projected to the boundaries of the potential, reaching a non-trivial topological insulator, characterized by an insulating bulk surrounded by highly entangled superfluid edges, which are topologically protected by a local particle-hole symmetry. We also find a semi-quantitative agreement between the superconducting order parameter and the single-site entanglement, confirming then that entanglement can be used as a topological marker and an order parameter in these systems. The charge gap not only confirms the transition from a superfluid to a non-trivial topological insulator, but also shows that this transition is mediated by a metallic intermediate regime within the bulk. Using the gap we could depict a phase diagram for which the non-trivial topological insulator can be found in such harmonically confined attractive systems. Our study enables progress in topological quantum information processing via confined fermionic systems.

ACKNOWLEDGMENTS

We thank fruitful discussions with F. Iemini, F. Assaad, G. Diniz, E. Vernek, R. Resta and M. Continentino. This research was supported by FAPESP (2021/06744-8; 2023/00510-0; 2023/02293-7) and CNPq (403890/2021-7; 140854/2021-5; 306301/2022-9).

Data Availability Statement – The data that support the findings of this study are available from the corresponding author upon reasonable request.

- ¹L. A. Oliveira and W. Chen, *Physical Review B* **109**, 094202 (2024).
- ²Z. Wang, F. Sun, X. Xu, X. Li, C. Chen, and M. Lu, *Thin-Walled Structures* **202**, 112111 (2024).
- ³D. Liao, J. Zhang, S. Wang, Z. Zhang, A. Cortijo, M. A. H. Vozmediano, F. Guinea, Y. Cheng, X. Liu, and J. Christensen, *Nature Communications* **15**, 9644 (2024).
- ⁴Z. Song, S.-J. Huang, Y. Qi, C. Fang, and M. Hermele, *Science Advances* **5**, eaax2007 (2019).
- ⁵J.-L. Tambasco, G. Corrielli, R. J. Chapman, A. Crespi, O. Zilberberg, R. Osellame, and A. Peruzzo, *Science Advances* **4**, eaat3187 (2018).
- ⁶M. A. Continentino, *Physica B: Condensed Matter* **505**, A1 (2017).
- ⁷I. Olaniyan, I. Tikhonov, V. V. Hevelke, S. Wiesner, L. Zhang, A. Razumayana, N. Cherkashin, S. Schamm-Chardon, I. Lukyanchuk, D.-J. Kim, and C. Dubourdieu, *Nature Communications* **15**, 10047 (2024).
- ⁸A. C. P. Lima, R. C. B. Ribeiro, J. H. Correa, F. Deus, M. S. Figueira, and M. A. Continentino, *Scientific Reports* **13**, 1508 (2023).
- ⁹J. Lee, N. Kang, S.-H. Lee, H. Jeong, L. Jiang, and S.-W. Lee, *Physical Review X Quantum* **5**, 030322 (2024).
- ¹⁰T. Dai, A. Ma, J. Mao, Y. Ao, X. Jia, Y. Zheng, C. Zhai, Y. Yang, Z. Li, B. Tang, J. Luo, B. Zhang, X. Hu, Q. Gong, and J. Wang, *Nature Materials* **23**, 928 (2024).
- ¹¹M. Zahid Hasan, S.-Y. Xu, D. Hsieh, L. Andrew Wray, and Y. Xia, in *Topological Insulators*, Contemporary Concepts of Condensed Matter Science, Vol. 6, edited by M. Franz and L. Molenkamp (Elsevier, 2013) pp. 143–174.
- ¹²F. D. M. Haldane, *Physical Review Letters*. **61**, 2015 (1988).
- ¹³C. L. Kane and E. J. Mele, *Science* **314**, 1692 (2006).
- ¹⁴P. B. Melo, S. a. A. S. Júnior, W. Chen, R. Mondaini, and T. Paiva, *Physical Review B* **108**, 195151 (2023).
- ¹⁵R. Bianco and R. Resta, *Physical Review B* **84**, 241106 (2011).
- ¹⁶M. A. Bandres, M. C. Rechtsman, and M. Segev, *Physical Review X* **6**, 011016 (2016).

- ¹⁷W. A. Benalcazar, B. A. Bernevig, and T. L. Hughes, *Physical Review B* **96**, 245115 (2017).
- ¹⁸T. Paiva, Y. L. Loh, M. Randeria, R. T. Scalettar, and N. Trivedi, *Physical Review Letters*. **107**, 086401 (2011).
- ¹⁹F. Schäfer, T. Fukuhara, S. Sugawa, Y. Takasu, and Y. Takahashi, *Nature Reviews Physics* **2**, 411 (2020).
- ²⁰C. Gross and I. Bloch, *Science* **357**, 995 (2017).
- ²¹M. Lewenstein, A. Sanpera, and V. Ahufinger, *Ultracold Atoms in Optical Lattices: Simulating Quantum Many-Body Systems*, 1st ed. (OUP Oxford, Oxford, UK, 2012) p. 490.
- ²²T. Pauletti, M. Sanino, L. Gimenes, I. M. Carvalho, and V. V. França, *Journal of Molecular Modeling* **30**, 268 (2024).
- ²³L.-A. Wu, M. S. Sarandy, and D. A. Lidar, *Physical Review Letters*. **93**, 250404 (2004).
- ²⁴L. Amico, R. Fazio, A. Osterloh, and V. Vedral, *Reviews of Modern Physics* **80**, 517 (2008).
- ²⁵T. Pauletti, M. Silva, G. Canella, and V. V. França, *Physica A: Statistical Mechanics and its Applications* **644**, 129824 (2024).
- ²⁶G. A. Canella and V. V. França, *Scientific Reports* **9**, 15313 (2019).
- ²⁷G. A. Canella and V. V. França, *Physica A: Statistical Mechanics and its Applications* **545**, 123646 (2020).
- ²⁸D. Arisa and V. V. França, *Physical Review B* **101**, 214522 (2020).
- ²⁹G. A. Canella, K. Zawadzki, and V. V. França, *Scientific Reports* **12**, 8709 (2022).
- ³⁰V. E. Korepin, *Physical Review Letters*. **92**, 096402 (2004).
- ³¹O. S. Zozulya, M. Haque, K. Schoutens, and E. H. Rezayi, *Physical Review B* **76**, 125310 (2007).
- ³²N. Laflorencie, *Physics Reports* **646**, 1 (2016).
- ³³H. Li and F. D. M. Haldane, *Physical Review Letters*. **101**, 010504 (2008).
- ³⁴T. P. Oliveira, P. Ribeiro, and P. D. Sacramento, *Journal of Physics: Condensed Matter* **26**, 425702 (2014).
- ³⁵M. Brzezińska, M. Bieniek, T. Woźniak, P. Potasz, and A. Wójs, *Journal of Physics: Condensed Matter* **30**, 125501 (2018).
- ³⁶S. Trebst and C. Hickey, *Physics Reports* **950**, 1 (2022).
- ³⁷S. V. Isakov, M. B. Hastings, and R. G. Melko, *Nature Physics* **7**, 772 (2011).
- ³⁸T. Giamarchi, *Quantum Physics in One Dimension*, 1st ed., International Series of Monographs on Physics, Vol. 121 (Clarendon Press, Oxford, 2003).
- ³⁹F. Marsiglio, *Physical Review B* **55**, 575 (1997).
- ⁴⁰X.-W. Guan, M. T. Batchelor, and C. Lee, *Reviews of Modern Physics* **85**, 1633 (2013).
- ⁴¹U. Schollwöck, *Annals of Physics* **326**, 96 (2011).
- ⁴²S. R. White, *Physical Review Letters*. **69**, 2863 (1992).
- ⁴³M. Fishman, S. White, and E. M. Stoudenmire, *SciPost Physics Codebases* , 004 (2022).
- ⁴⁴J. P. Coe, V. V. França, and I. D'Amico, *Europhysics Letters* **93**, 10001 (2011).
- ⁴⁵V. V. França and K. Capelle, *Physical Review Letters*. **100**, 070403 (2008).
- ⁴⁶V. V. França and I. D'Amico, *Physical Review A* **83**, 042311 (2011).
- ⁴⁷J. P. Coe, V. V. França, and I. D'Amico, *Physical Review A* **81**, 052321 (2010).
- ⁴⁸V. V. França, *Physica A: Statistical Mechanics and its Applications* **475**, 82 (2017).
- ⁴⁹G. A. Canella and V. V. França, *Physical Review B* **104**, 134201 (2021).
- ⁵⁰T. Kaneko, T. Shirakawa, S. Sorella, and S. Yunoki, *Physical Review Letters*. **122**, 077002 (2019).
- ⁵¹M. Qin, C.-M. Chung, H. Shi, E. Vitali, C. Hubig, U. Schollwöck, S. R. White, and S. Zhang, *Physical Review X* **10**, 031016 (2020).
- ⁵²K. S. Huang, Z. Han, S. A. Kivelson, and H. Yao, *npj Quantum Materials* **7**, 17 (2022).
- ⁵³A. E. Feiguin and F. Heidrich-Meisner, *Physical Review B* **76**, 220508 (2007).
- ⁵⁴V. V. França, D. Hördlein, and A. Buchleitner, *Physical Review A* **86**, 033622 (2012).
- ⁵⁵M. Rigol and A. Muramatsu, *Physical Review A* **70**, 031603 (2004).
- ⁵⁶P. Sengupta, M. Rigol, G. G. Batrouni, P. J. H. Denteneer, and R. T. Scalettar, *Physical Review Letters*. **95**, 220402 (2005).
- ⁵⁷F. Pollmann, A. M. Turner, E. Berg, and M. Oshikawa, *Physical Review B* **81**, 064439 (2010).
- ⁵⁸J. I. Cirac, D. Pérez-García, N. Schuch, and F. Verstraete, *Reviews of Modern Physics* **93**, 045003 (2021).
- ⁵⁹F. Pollmann and A. M. Turner, *Physical Review B* **86**, 125441 (2012).
- ⁶⁰X.-L. Qi and S.-C. Zhang, *Reviews of Modern Physics* **83**, 1057 (2011).
- ⁶¹H. Hu, S. Chen, T.-S. Zeng, and C. Zhang, *Physical Review A* **100**, 023616 (2019).